Double Chooz: Muon Reconstruction

Leela Chakravarti
Johns Hopkins University
Nevis Laboratories, Columbia University

August 6, 2009

Abstract

This paper describes work done on the Double Chooz neutrino detection project at Columbia University's Nevis Labs during the summer of 2009. Presented in this paper are studies done on elimination of background events in the experiment. Cables for the outer veto system that reduces background were put together and tested for systematic errors. This report also describes studies of reconstruction accuracy of muons and changes based on different starting energies and positions in the detector and possible explanations of observed trends.

1 Introduction

1.1 The Standard Model

The Standard Model, which describes elementary particles and their interactions, is at present the most widely accepted theory in particle physics, resulting from decades of experimentation and modification. However, it still does not provide a complete explanation of various phenomena. One main issue is that the theory only accounts for the electromagnetic, strong nuclear and weak nuclear forces, excluding the fourth fundamental force of gravity.

The model consists of force carrier particles known as bosons, along with two main groups of fermions, quarks and leptons. Fermions are thought to be the building blocks of matter, while bosons mediate interactions between them. All fermions have corresponding antiparticles with equal mass and opposite charge. Quarks have fractional charge and interact via the strong force; they combine to form hadrons, like neutrons and protons. Up and down quarks form neutrons and protons, while quarks in the other two generations are generally unstable and decay to particles of lesser mass. Of the leptons, three are charged and three are electrically neutral, and all have spin 1/2. The electron, muon, and tau all have a charge of -1, though the muon and tau are much more massive than the electron, and thus have short lifespans before they decay. Each charged lepton corresponds to a neutral, much lighter neutrino particle.

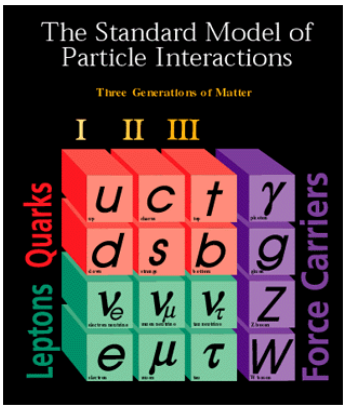

Figure 1: Standard Model in Particle Physics [2]

1.2 Neutrinos and Oscillations

The existence of the neutrino was proposed by Wolfgang Pauli as an explanation for the experimental result of beta decay of a neutron into a proton, which showed that the electrons emitted in the decay have a range of energies, rather than a unique energy. [7] The electrons also do not seem to take the total energy that they are allotted, suggesting that there is another particle emitted that makes up for these discrepancies. The neutrino, thought to be massless, left-handed (counterclockwise spin), uncharged, and weakly interacting, was thus introduced. However, experiments have shown that this description is not entirely correct.

Through conservation of Lepton Family Number in the Standard Model, neutrinos cannot change flavor; an electron neutrino cannot become a muon neutrino or a tau neutrino. [5] Through the weak force, an electron and electron neutrino can transmute into each other, but particles cannot directly change families. A tau cannot directly decay into an muon without production of a tau neutrino. Despite this prediction, neutrinos do appear to oscillate and change flavors. For example, as an electron neutrino moves through space, there is a chance that it will become a muon or tau neutrino. This implies that mass states and flavor states are not the same, as previously thought, and neutrinos actually do have small masses. The waves of two different mass states interfere with each other, forming different flavor states, creating an oscillation probability for one neutrino to change flavors. In the case of electron and muon neutrinos, this probability is:

$$P_(\nu_\mu \rightarrow \nu_e) = sin^2(2\theta)sin^2(\frac{1.27\Delta m^2 L}{E}) \quad (1)$$

where ν_μ and ν_e are the different flavors, Δ m is the difference in mass of the two particles, E is the energy, θ is the mixing angle, and L is the distance between the production and detection points of the neutrino. The different neutrino flavor states are different combinations of mass states (ν_1, ν_2, and ν_3), and the transition from one basis to the other is described by a mixing matrix. In the three-neutrino case, the transition is described by a unitary rotation matrix that relates flavor eigenstates to mass eigenstates. [6]

$$\begin{pmatrix} \nu_e \\ \nu_\mu \\ \nu_\tau \end{pmatrix} = \begin{pmatrix} U_{e1} & U_{e2} & U_{e3}e^{i\delta} \\ U_{\mu 1} & U_{\mu 2} & U_{\mu 3} \\ U_{\tau 1} & U_{\tau 2} & U_{\tau 3} \end{pmatrix} \begin{pmatrix} \nu_1 \\ \nu_2 \\ \nu_3 \end{pmatrix} \quad (2)$$

This matrix can be split into three matrices, each of which deals with a different mixing angle. [1]

Two of the angles, θ_{12} and θ_{23} have been determined by experiments with solar and atmospheric neutrinos, but θ_{13} is still undetermined, with only an upper limit of 13^o. Various efforts, such as the Double Chooz project, are underway to try determine this last angle and better understand the way that neutrinos oscillate.

1.3 Double Chooz

Double Chooz is a neutrino detection experiment located in the town of Chooz in northern France. Instead of studying solar or atmospheric neutrinos, this project focuses on neutrinos produced at two nuclear reactors. Through fission reactions of isotopes U-235, U-238, Pu-239 and Pu-241, electron antineutrinos are produced and move in the direction of two detectors. The original Chooz experiment only had one detector, but Double Chooz plans to achieve higher sensitivity and accuracy by using both near and far detectors and looking for changes in antineutrino flux from the near to the far. The use of two detectors corrects for uncertainties about the absolute flux and the location of the experiment because the two identical detectors are compared to each other and only differ on how far away each one is from the reactors. Assuming that oscillations will change some electron antineutrinos into other flavors, there should be less electron antineutrinos observed at the far detector than at the near. Should this effect be observed, the probability can be calculated and using equation 1, the value of $sin^2(2\theta_{13})$ can also be determined.

The near detector is 410km away from the reactors, while the far detector is 1.05km away. Both detectors are identical, with main tanks filled with scintillator material doped with gadolinium [4]. When an electron antineutrino particle reaches either detector, it reacts according to inverse beta decay:

$$\overline{\nu_e} + p \rightarrow e^+ + n \quad (3)$$

In each tank, there are about 6.79 x 10^{29} protons for the electron antineutrinos to react with. The actual detection of the particle is a result of the products of the inverse beta decay reaction.

First, the positron produced annihilates with an electron, emitting two photons about 0.5 MeV of energy each. The neutron then gets captured on a gadolinium nucleus after about 100 μs, emitting several photons with a total energy of around 8

[1]

$$U = \begin{pmatrix} cos(\theta_{12}) & sin(\theta_{12}) & 0 \\ -sin(\theta_{12}) & cos(\theta_{12}) & 0 \\ 0 & 0 & 1 \end{pmatrix} * \begin{pmatrix} cos(\theta_{13}) & 0 & e^{-i\delta_{CP}}sin(\theta_{13}) \\ 0 & 1 & 0 \\ e^{-i\delta_{CP}}sin(\theta_{13}) & 0 & cos(\theta_{13}) \end{pmatrix} * \begin{pmatrix} 1 & 0 & 0 \\ 0 & cos(\theta_{23}) & sin(\theta_{23}) \\ 0 & -sin(\theta_{23}) & cos(\theta_{23}) \end{pmatrix}$$

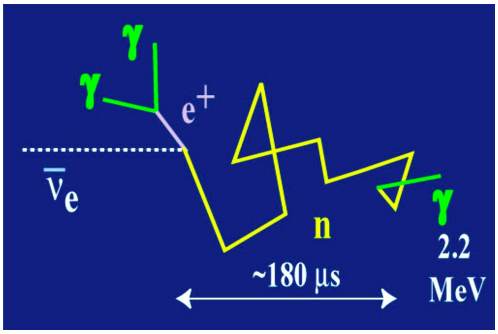

Figure 2: Inverse Beta Decay Reaction [1]

MeV. The signals emit light, which is then detected by several photomultiplier tubes (PMTs) around the inner surface of the tank. This double signal with the appropriate time lapse indicates the presence of an electron antineutrino.

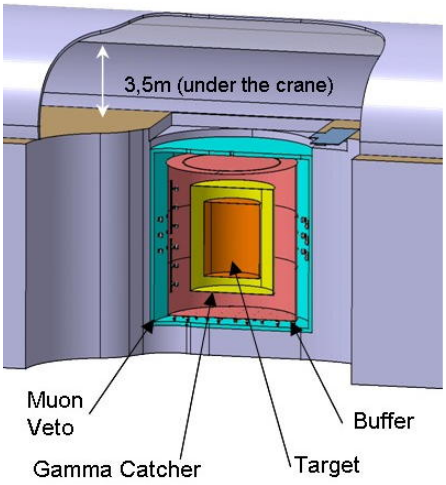

Figure 3: Double Chooz detector vessel

Each detector has many layers and components. The central region is a tank filled with 10.3 m^3 of scintillator. Moving outward, the gamma catcher region provides extra support for detecting the neutron capture signal. Surrounding the gamma catcher is the buffer region, where the 534 8-inch PMTs are located. Finally, the inner and outer veto systems are in place to help decrease background signal by other particles, such as muons or neutrons.

2 Muon Background and Reconstruction

2.1 Muon Background

One of the main sources of background events and causes of error in the Double Chooz experiment is the effect of cosmic ray muons, along with gamma, beta and neutron signals in the detector and rock. Near-miss muons in the rock around the detector react and form fast neutrons, which go through the detector and create false signals. Muons produce neutrons in detector through spallation (collision of high energy particle with a nucleus) and muon capture. Recoil protons from interacting neutrons are mistaken for positrons, and successive neutron capture confirms the false antineutrino signal. Muons can also make it into the detector and cause such background signals. In order to properly reject these signals, it is important to know which specific signals to ignore.

2.2 Outer Veto and Cabling

One of the ways to reduce error due to muon background is to use an outer veto system, which identifies muons that can produce backgrounds in the detector. Once these specific muons are tagged, the signals they produce can be eliminated from the data set. The outer veto detector differentiates between muons that go through target and those that pass near the target. It also detects muons that may miss the inner veto completely or may just clip the edges of the inner veto. The outer veto is composed of staggered layers of scintillator strips above the detector. Strips in the X and Y directions can measure coincidence signals and identify muon tracks. Signals from light created in the scintillator are sent to PMTs, which process the signals in a similar fashion to the main detector.

Arrival of event signals should be properly timed to minimize dead time for the detector, delay time of the signal and to preserve the pulse signal. Cables that carry the signals must therefore be made uniformly and within these specifications, also taking into account the physical distance that must be traversed. Different types of cables offer different capabilities for data transfer. The outer veto uses RG58 and RG174 cables for data transfer. Each type of cable has a different characteristic delay time per foot, which must be accounted for to understand the total delay time for the signal. 50-foot and 61-foot RG174 cables were cut, and will be combined with 110-foot and 97.5-foot RG58 cables for data transfer in the upper and lower sections of the outer veto. RG58 cable must be used in addition to RG174 because the use of only RG174 would result in a degeneration of the signal along the cable, as RG174 has a lower bandwidth and less capacity for data. The overall delay should be around 270 ns, and the cables must be tested for their individual delay times to ensure that this value remains constant for all cables to avoid systematic errors. RG174 sections of the outer veto cables have three cables bound together, one for the Clock, one for the Trigger, and one for the Gate. It is especially important that the Gate cable have the correct delay time, because it mediates data collection at certain intervals.

Cables for the outer veto were tested for proper delay times using an oscilloscope. Each end of the cable connects to an input channel in the oscilloscope, and the difference

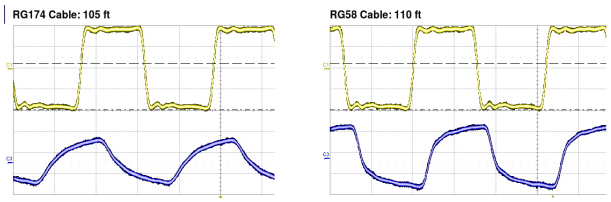

Figure 4: Waveforms: Signal is better preserved along RG58 cable

in timing of pulse appearance is the delay time. It is apparent from the waveforms shown that there is a greater degeneration of the signal when using only RG174.

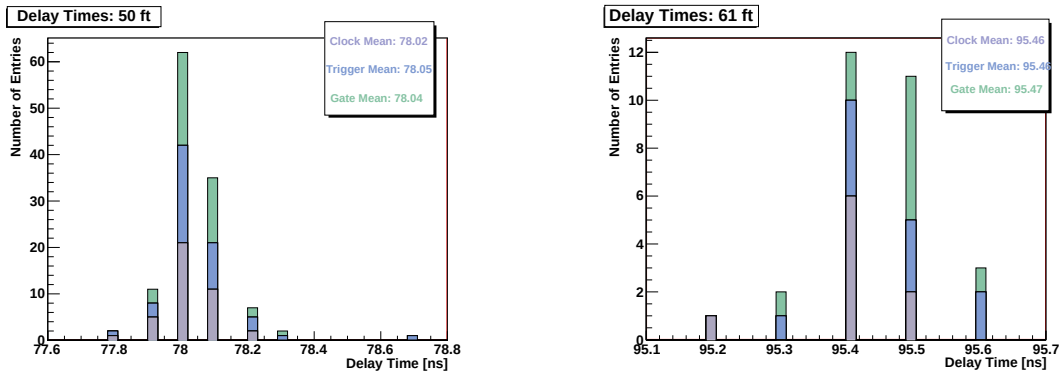

(a) 50-ft. cable

(b) 61-ft. cable

Figure 5: RG174 cable delay times

For the RG174 cable, cable lengths of 50 feet should have a delay time between 76 and 81 ns, while 61-foot cables should have delay times between 93 and 99 ns. Plots of delay times indicate that all of the cables made for the outer veto have delay times within the expected ranges. These cables will be put into place in the final construction of the outer veto detector.

2.3 Simulation: DOGS Overview

Muons that make it into the detector and past the outer veto must be accounted for and identified. The muon-caused signals can be determined by muon location in the detector, as the signals are predicted to occur within some distance from muon location, depending on energy and position of the muons. Simulation software is used to imitate muons passing through the detector and the reconstruction of the muons starting positions and energies. Various algorithms and simulation processes are run through in order to reconstruct particles in the detector. The Double Chooz collaboration uses a software package called Double Chooz Offline Group Software, or DOGS. Within DOGS, there are basic simulation scripts that generate different types of particles, study them through the detector, and reconstruct their properties, such as type, starting position, and starting energy or momentum. The DOGS simulation keeps track

of how much energy is deposited where, other particles produced due to the original particles, signals detected at different photomultiplier tubes, time between signals, and track directions, among other things. All of this information is stored and can later be accessed for analysis.

2.4 Data Flow in Muon Simulation

In order to work with DOGS and produce specific simulations, it is often necessary to modify the skeleton scripts that are originally provided to meet different needs. DOGS uses a software called GEANT4 to generate particles and simulate their activity in a liquid scintillator detector. GEANT4 simulations take into account the geometry of the detector, the specific materials used, particle location with respect to the detector, optical photons, and properties of photomultiplier tubes.

For this simulation of muons in the detector, one of the particle generator scripts was modified to include a generator gun, which allows for specification of particle type, the number of particles, production rate, starting position, initial momentum and energy. If energy is given, momentum is treated as directional only, to avoid over specification of the problem. The generator script also has information about whether or not photons and the Cerenkov light effect are included.[2] In order to produce proper scintillation light for PMT detection, photons and Cerenkov light are activated. The script is run in DCGLG4sim, which is the Double Chooz version of the GEANT4 simulation. All information about the particles is used by following simulation scripts to show a response to the particle and then to reconstruct its original information.

After particles are generated using DCGLG4sim, the output of the generation and particle tracking information is sent to the Double Chooz Readout Simulation Software, or DCRoSS. DCRoSS models the detectors response to the particles, from signal detection and amplification at the photocathode on the PMTs to data acquisition based on varying trigger levels depending on the expected signal strength. Within RoSS scripts, PMT and data acquisition settings are changed to accommodate specific simulations.

Finally, the output from DCRoSS is channeled into a Double Chooz Reconstruction, or DCReco script. DCReco runs through reconstruction algorithms (discussed in the following section) to determine properties of the particles, such as spatial information and initial energy. It uses the information from DCRoSS about location and magnitude of deposited energy in the detector to reconstruct particle information.

Output from each step of the simulation is stored in different Info Trees, and can be accessed in order to compare differences between actual and reconstructed information or look at where energy was deposited in the detector. Variables in Info Trees are accessed through the use of ROOT, a data analysis framework created to handle large amounts of data. A study of reconstruction efficiency as a function of starting energies and positions was thus conducted.

[2]Charged particles traveling through a medium in which their speed is greater than the speed of light in that medium disrupt the electromagnetic field and displace electrons in atoms of the material. When the atoms return to ground state, they emit photons; this is known as the Cerenkov effect.

3 Reconstruction Accuracy

3.1 Reconstruction Algorithms

Muon spatial and energy reconstruction in the detector is based on a maximum likelihood algorithm that combines available information about an event. The characterization of an event is a function of seven parameters, namely the (x, y, z, t) four-dimensional vertex vector, the directional vector (ϕ, θ), and the energy E [4]:

$$\overrightarrow{\alpha} = (x, y, z, t, \phi, \theta, E) \tag{4}$$

The likelihood of an event is the product over the individual charge and time likelihoods at each of the PMTs:

$$L_{event} = \prod_{i=1}^{N_{PMTs}} L_q(q_i; \overrightarrow{\alpha}) L_t(t_i; \overrightarrow{\alpha}) \tag{5}$$

Given a set of charges q_i and corresponding times t_i, L_{event} is the probability that the event has the characteristics given by the seven-dimensional vector, $\overrightarrow{\alpha}$. Reconstruction looks for a maximization of L_{event} to determine what specific combination of vertex, direction and energy corresponds to the event. DCReco uses the above method to reconstruct muon information. Because the process uses a likelihood algorithm, reconstruction is based on a probability and therefore will not always yield the same results, even if original particles had the same information. The accuracy of this algorithm may also change depending on starting positions and starting energies.

3.2 Different Starting Energies

To assess reconstruction efficiency and overall accuracy, it is necessary to test different original particle information. In this study, starting energies and positions were changed to look for efficiency trends. Different starting energies to use were determined through consideration of the energy spectrum of muons. All of the muons tested at different energies had the same starting position in the detector at a radius of 500 mm from the center at the top of the target region.

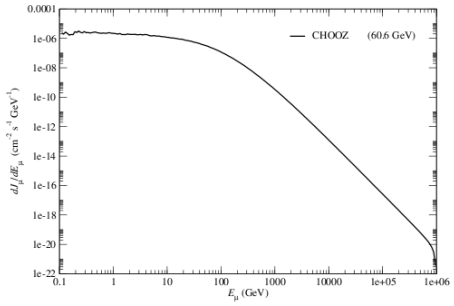

Figure 6: Energy spectrum of muons from Double Chooz proposal [4]

The tested energies were in the range of 1 GeV to about 25 GeV. This range corresponds to the section on the energy spectrum before the change in muon flux with respect to changing energy starts to decrease. Having energy range over different orders of magnitude helped show trends on a grander scale. About seven different energies were tested for trends in reconstruction efficiency. Because the reconstruction algorithm takes into account energy detected at each PMT (in terms of charge), there could be a correlation between energy amounts and efficiency.

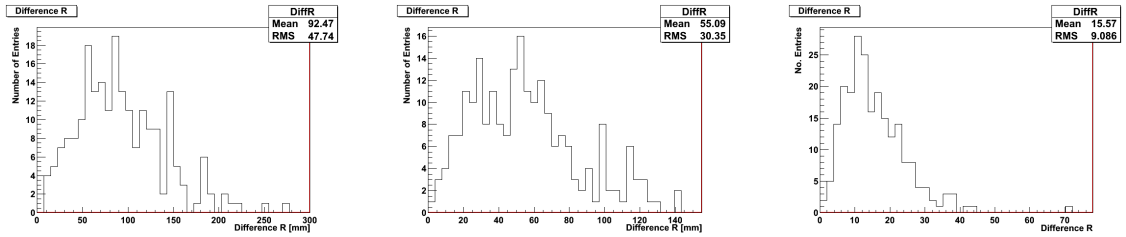

(a) E: 1000 MeV (b) E: 7500 MeV (c) E: 25000 MeV

Figure 7: RMS and mean values: difference of reconstructed and truth R positions

Plots of the difference between reconstructed radial position and actual radial position show that both the mean and RMS values decrease with increasing energy. Histogram width and deviation gets smaller as energy increases and the reconstruction algorithms seem to get closer to predicting the actual starting position. The RMS value at 25000 MeV is about 1/5 the value at 1000 MeV.

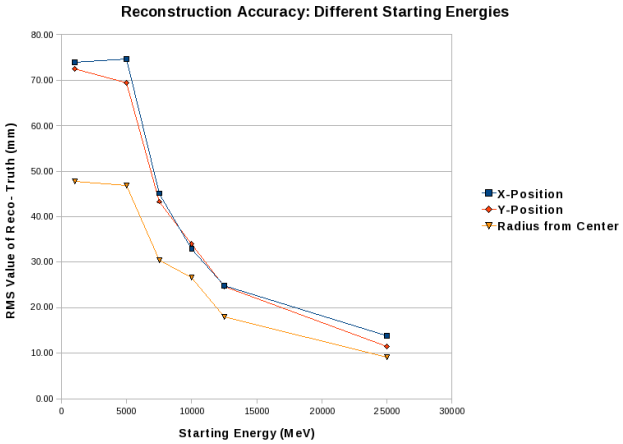

Figure 8: RMS Values at changing energies

Including all tested energies indicates that there is a noticeable drop in RMS value of the difference in reconstructed and truth positions and thus an increase in accuracy as energy increases. The effect of multiple Coulomb scattering as a particle goes through material could be responsible for this trend. Muons with lower initial energies and thus less momenta will not pass as easily through the detector, and the path may deflect

because of multiple scattering off nuclei. This would result in a less well-defined path displayed by hits at the PMTs and a less accurate reconstruction of position. This idea is tested by calculating deflection angle θ_0 at the different energies, using the formula:

$$\theta_0 = \frac{13.6MeV}{\beta cp} z\sqrt{x/X_0}[1 + 0.038ln(x/X_0)] \tag{6}$$

where where βc is velocity of the muon, p is the momentum, and x/X_0 is the thickness of the scattering medium [3]. The value of x/X_0 is calculated from the ratio of the track length to the radiation length in that material.[3] Momentum of a relativistic particle is:

$$p = \sqrt{\frac{E^2}{c^2} - (m_0 c)^2} \tag{7}$$

and at high energies, is essentially equal in magnitude to the energy. The coefficient β for the c (the speed of light in a vacuum) is calculated using the equation:

$$\beta = \frac{cp}{E} \tag{8}$$

which considers starting energy and momentum. The theoretical deflection angle θ_0 was calculated for each starting energy. Using $tan(\theta_0)$ and scaling for the height of the tank results in a comparable value in units of length to the RMS values previously shown.

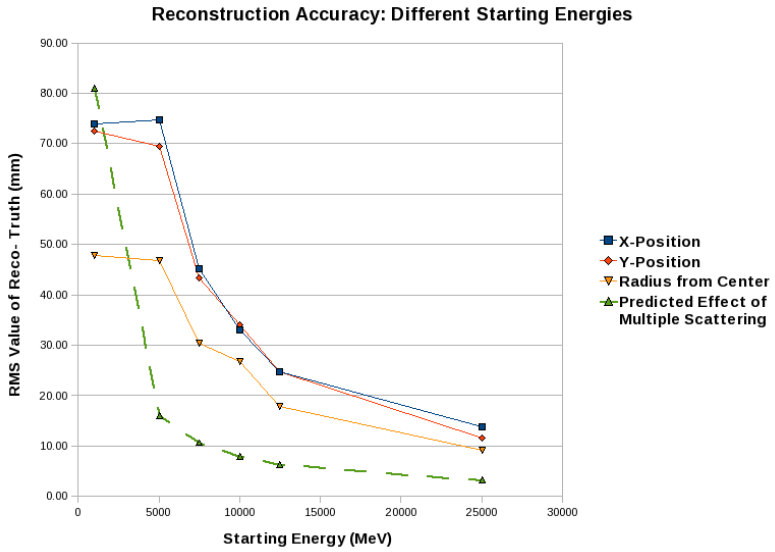

Figure 9: Multiple scattering prediction

The plot originally shown now includes the prediction of multiple scattering. Although the trend does not appear exactly identical, the result that the observed data

[3]Radiation length is defined as the mean path length required to reduce the energy of relativistic charged particles by the factor 1/e, or 0.368, as they pass through matter.

and theoretical prediction are on the same order of magnitude and in the same approximate range shows that they could correspond. Plotting this range at the varying starting energies indicates that it is likely that multiple scattering produces the results seen, and the effect of this on reconstruction accuracy should be accounted for when considering different energy muons.

3.3 Different Starting Positions

Muons starting at different distances from the center of the detector were also considered. In each run, muons were generated at the top of the detector so that they are through-going. Runs with varying radii from the center changed the x-position based on different sections of the detector.

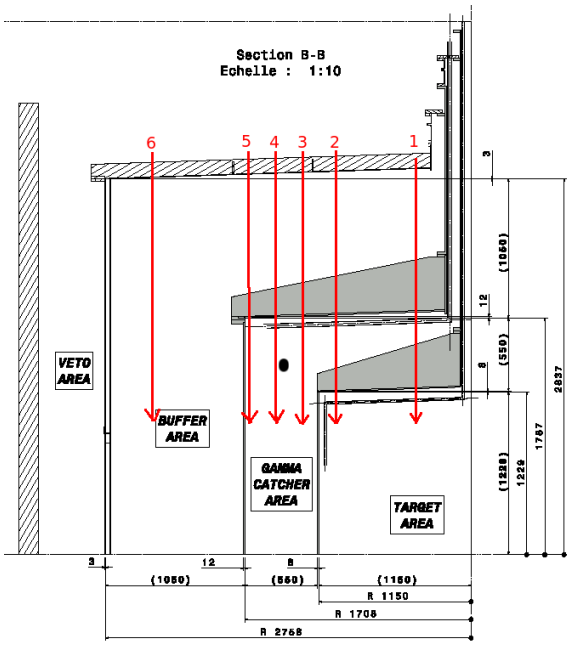

Figure 10: Various starting positions in detector [4]

According to the diagram, x-position was changed to cover each different section, as well as tracks in the middle of sections and close to the walls, to see if PMT response changes when the particles are very close to the walls. Simulations took place in the middle of the target region (1), close to the wall on the target side (2), close to the wall on the gamma catcher side (3), in the middle of the gamma catcher region (4), close to the wall on the gamma catcher side before the buffer area (5), and through the buffer area (6).

As a preliminary check, a plot of the energy deposited in the detector's central region shows that the particles are being generated according to the position specifications. There is a slight peak in the gamma catcher region where the muons go through the most scintillating volume. The buffer region, which is non-scintillating, should not

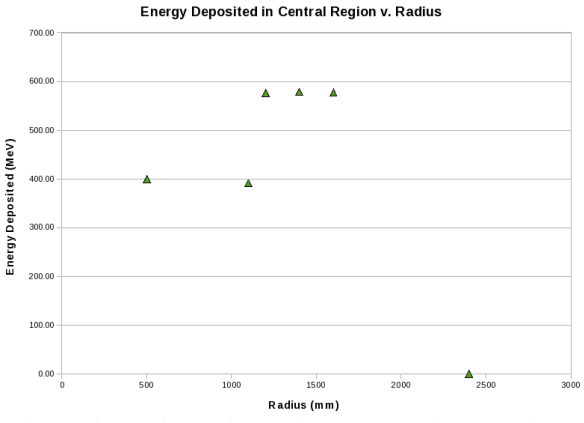

Figure 11: Energy deposited in central region of detector

detect any energy, which is also observed. The range of values for energy deposited also matches up with the expected energy loss rate of about 2.3 MeV/cm in the tank.

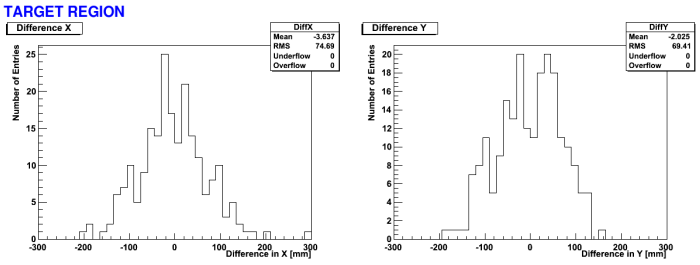

(a) Target Region

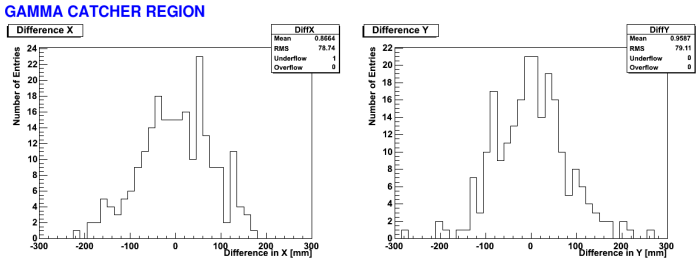

(b) Gamma Catcher Region

Figure 12: X and Y positions: difference between reconstructed and truth

Plots of differences in X and Y position reconstruction show that muons going through the target region are reconstructed slightly better than those going through the gamma catcher region. Comparing differences between reconstruction and truth starting positions shows that accuracy decreases when muons go through the gamma catcher region or near vessel walls. This effect could be due to changes in PMT response. Additional testing at more positions would give a more precise indication of

whether or not PMT response is affected by muons that pass very close to the walls.

Figure 13: RMS values at changing positions

A general decrease in accuracy appears in the gamma catcher region when all positions are considered. Other areas of the detector show a fairly consistent reconstruction accuracy. Muons starting either in the target or outer regions seem to be reconstructed to within approximately 50 mm of the truth vertex.

4 Conclusions

Identifying and rejecting background is an important part of data collection in Double Chooz. When background rates are accounted for, data collection becomes much more efficient. The use of hardware devices like the Outer Veto make this possible in the actual data collection. Outer veto cabling tests indicate that the delay times and signal degeneration are within acceptable ranges. In analysis, reconstruction algorithms are important for understanding locations of background signals and tagging specific false events. Studies of muon reconstruction in the DOGS package give information about the software's accuracy as well as how it can be used to assist in analysis of real data. Reconstruction accuracy appears to decrease in Gamma Catcher region and close to vessel walls, possibly due to changes in PMT response. Reconstruction accuracy appears to increase with starting energy, likely due to the effect of multiple scattering at lower energies. Although these trends are observed in this study, higher statistics runs at additional energies and positions would provide a more definitive analysis to extend this initial study.

5 Acknowledgments

I would like to extend a sincere thanks to project advisors Mike Shaevitz, Leslie Camilleri, Camillo Mariani and Arthur Franke for their help and guidance on my work, as well as to everyone else who worked with me on Double Chooz this summer for support and input. I would also like to thank the National Science Foundation for providing me with the wonderful opportunity to work at Nevis this summer.

References

[1] Inverse beta decay, http://theta13.phy.cuhk.edu.hk/pictures/inversebetadecay.jpg.

[2] Standard model, http://www.fnal.gov/pub/inquiring/timeline/images/standardmodel.gif.

[3] C. Amsler et. al (Particle Data Group). Passage of particles through matter. Physics Letters B667(1), 2008.

[4] F. Ardellier et al. (Double Chooz Collaboration). Proposal. *arXiv:hep-ex/0606025*, 2006.

[5] J. Kut. Neutrinos: An insight into the discovery of the neutrino and the ongoing attempts to learn more. 1998.

[6] M. Shaevitz. Reactor neutrino experiment and the hunt for the little mixing angle, 2007.

[7] R. Slansky et al. The oscillating neutrino: an introduction to neutrino masses and mixing. *Los Alamos Science*, 25:28–72, 1997.